DETAILED MEASUREMENTS IN AN IDEALIZED AND A PRACTICAL NATURAL GAS HOUSEHOLD BOILER

MESURES DETAILLEES DANS UN CHAUDIERE MODELE ET UNE CHAUDIERE COMMERCIALE AU GAZ NATUREL

P.F. Miquel, N. Larass and M. Perrin
Direction de la Recherche, Gaz de France, France

F. Lasagni and M. Beghi
Worgas Bruciatori s.r.l., Italy

S. Hasko and M. Fairweather
BG Technology, United Kingdom

G. Hargrave and G. Sherwood
University of Loughborough, United Kingdom

H. Levinsky, A.V. Mokhov and H. de Vries
N.V. Nederlandse Gasunie, The Netherlands

J.P. Martin, J.C. Rolon, L. Brenez and P. Scouflaire
CNRS-EM2C, Ecole Centrale Paris, France

D.I. Shin, G. Peiter, T Dreier and H.R. Volpp
PCI, University of Heidelberg, Germany

ABSTRACT

The results of an experimental study of the combustion processes in an idealized boiler are presented. This experimental study was part of a project supported by the European Community (Brite-Euram III program) which aimed at developing tools for the design of clean and efficient household boilers. The idealized boiler was designed with an optically accessible combustion chamber and independent controls of power input, primary and secondary aerations. Combustion processes were investigated by combined measurements of temperature, velocity, mean species concentrations and radical concentrations using probe sampling and non-intrusive optical techniques. Measurements were obtained for five different flame cases. Results focused on understanding the pollutant formation mechanisms in these five flames. The work reported here represents one of the first comprehensive studies of combustion processes in a practical boiler.

RESUME

Cette publication présente les résultats de l'étude expérimentale des processus de combustion dans une chaudière domestique modèle. Cette étude expérimentale représente l'une des tâches d'un projet co-financé par la Communauté Européenne (programme Brite-Euram III) dont l'objectif est de développer des outils d'aide à la conception de chaudières domestiques à haut rendement et faible émission de polluants. La chaudière modèle a été conçue avec une chambre de combustion optiquement accessible et un contrôle indépendant de la puissance et des taux d'aération primaires et secondaires. Les processus de combustion ont été étudiés par mesures combinées de température, de concentration d'espèces chimiques stables et radicalaires, et de vitesses grace à des sondes de prélèvement et par des techniques optiques. Ces mesures ont été effectuées sur 5 cas-tests différents. Les résultats portent sur la compréhension des mécanismes de formation de polluants dans ces 5 cas-tests. Ces travaux représentent l'une des premières études des processus de combustion dans une chaudière domestique.

INTRODUCTION

Laminar premixed combustion has been widely studied by others as a basic combustion research problem (1-4). Nevertheless, up to now, few studies were devoted to laminar partially premixed flames with natural gas and operating conditions pertaining to practical devices (5,6). This lack of basic knowledge is restraining the understanding of stabilization and pollutant emission mechanisms in household boilers. This basic knowledge is required today to meet the increasingly stringent regulations on NO_x emissions limits. For instance, although NO_x emissions for most of the natural gas powered household boilers sold in Europe are currently around 120 mg/kWh (7), the European standards are moving towards lower limits, i.e., 50 mg/kWh.

Over the years, burner manufacturers have developed rules of thumb for choosing combination of design parameters, such as primary fuel-air ratio, port loading, and port spacing, to meet the approved specifications. However, this approach is a global one, where all measurements are made at the input and output of the appliance. This often results in unwanted effects such as the increase in CO emissions or decrease in flame stability which occur as NO_x emissions are reduced. Since the formation of pollutants in combustion systems depends upon the details of the combustion process itself, insights into these details are required for proper design of the appliance.

In a project supported by the European Community in the framework of the Brite-Euram III program, detailed measurements in the combustion chamber of an idealized household boiler were obtained. The objective was to understand, using advanced measurement techniques, how burner operation affects combustion performance and how this understanding can be used for improving boilers and burners. It was also to identify and develop measurement tools most adapted to boiler design aids. To that effect probe measurements were compared with measurements obtained using non-intrusive techniques. Finally, these detailed measurements were also used to provide an accurate and reliable database for validating numerical models also developed in the framework of the project.

The idealized boiler was developed with the same characteristics as that of a commercial boiler but with a simplified 2-dimensional geometry. Global measurements in the exhaust of the boiler were obtained and compared with measurements performed in a commercial boiler. Five different flame regimes were also selected. For the five regimes temperature, velocity, chemical species concentrations and flame emission measurements were obtained in the combustion chamber of the idealized boiler. Preliminary results are presented.

EXPERIMENTAL SETUP

Idealized Boiler and Operating Conditions

Most commercially available natural gas domestic boilers use laminar partially or totally premixed burners. They are made of different bars or blades with numerous small slots and holes, creating a complex 3-dimensional flow. To simplify this geometry, an idealized boiler was designed with a 2-dimensional flow. A schematic of this boiler is shown in Figure 1. The idealized boiler is a modified version of a commercial wall mounted boiler. Although its characteristics are similar to those of a commercial boiler in terms of power density and performance, it differs by the fact that the primary air, the secondary air, and the gas flow rates, hence the aeration ratio and power input, are controllable independently. The combustion chamber of the boiler was designed to allow optical-free access to the flame and the post combustion zones. Hence, non-intrusive measurement techniques can be used.

In the idealized boiler, the premixed air/gas mixture enters through a laminarization tank. It is then introduced into the combustion chamber through 7 identical slots (also called "primary channels"). The primary channels are filled with a bed of glass beads, 2 mm in diameter, and several fine stainless steel grids to ensure a laminar and uniform flow. The cross-section area of the primary channel at the burner mouth is 150 mm long by 3 mm wide. A secondary air stream is introduced through the 8 corresponding inter-blade channels (called "secondary channels"). A honeycomb structure and a stainless steel grid placed at the bottom of the boiler's body also ensures a uniform and laminar secondary air flow. The primary and secondary air flow rates and the gas flow rates are controlled by calibrated mass flow meters.

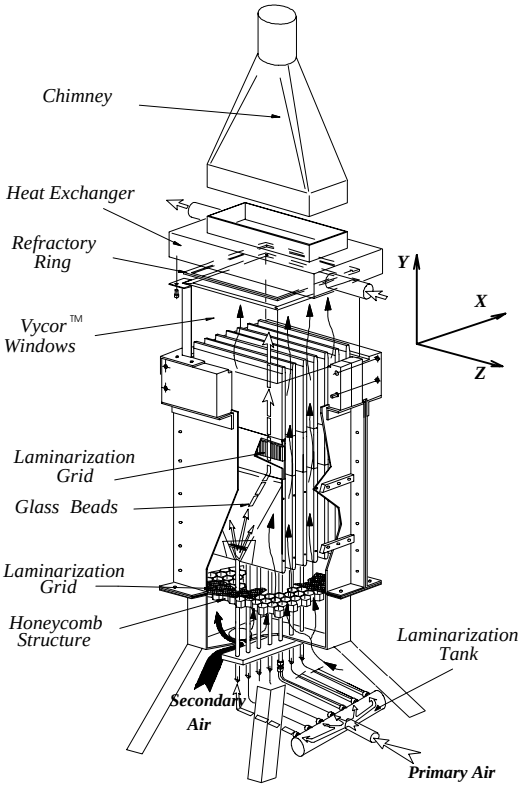

Figure 1. Schematic of the idealized boiler.

The combustion chamber (150 x 115 x 150 mm) is protected from entrainment of surrounding air by 4 glass (Vycor™) windows, held in place by 4 stainless steel mounts. A heat exchanger made of copper fins is placed on the top edges of the windows. This heat exchanger was designed to support a maximum load of 11 kW (Gross Calorific Value) with minimum pressure drop and to have an efficiency similar to that of commercial boilers. It was operated with an inlet water temperature of 60°C and an outlet water temperature of 65°C for all flame conditions investigated. A chimney is placed on top of the heat exchanger for flue gases exhaust. The composition of the flue gases was measured with a probe consisting of a copper tube located at the top of the chimney.

The combustion chamber is characterized by the X, Y, and Z axis (see Figure 1). The X axis is the horizontal axis which runs across the burner slots. The location at X = 0 mm corresponds to the center of the central slot. The slots being 16 mm apart, their centers are located at X = -48, -32, -16, 0, +16, +32, and +48 mm. The Y axis is the vertical axis (Y = 0 mm corresponds to the surface of the burner slot, and Y = 150 mm corresponds to the bottom of the heat exchanger). Last, the Z axis is the horizontal axis that runs along the burner slots (Z = 0 mm corresponds to the center of the slot).

In order to study the combustion mechanisms in the idealized boiler, two levels of measurements were performed: global measurements in the flue gases and detailed measurements in the combustion chamber. The overall measurements consisted of varying the primary aeration ratio, the secondary aeration ratio, and the power input independently, and measuring the NO_x and CO emissions at the flue gas probe. For the detailed measurements in the combustion chamber, five operating conditions referred to as « test cases » were defined. They are shown in Table 1. In all cases selected, the total aeration ratio was set to 1.4 and the power input was set to 10 kW. Case 1 and 2 have the same primary and secondary aeration ratio but a different fuel composition: natural gas like blend vs. pure methane, respectively. Case 3 uses pure methane with no secondary air (i.e.,

fully premixed flame). Finally, Case 4 and 5 have the same aeration ratios and fuel composition but differ by their flame type: in Case 5 a metal insert is placed inside the primary channel to create a V-shaped flame.

Table 1. Test cases selected as operating conditions for the idealized boiler.

Test Case	Fuel Composition			Fuel GCV ($kWh/m^3(n)$)	Flame Type	Primary Aeration	Second. Aeration
	CH_4	C_2H_6	C_3H_8				
1	0.9	0.06	0.04	11.04	Bunsen	0.6	0.8
2	1	0	0	9.87	Bunsen	0.6	0.8
3	1	0	0	9.87	Bunsen	1.4	0
4	1	0	0	9.87	Bunsen	1.2	0.2
5	1	0	0	9.87	V shaped	1.2	0.2

Commercial Boiler

The combustion performances of the idealized boiler were compared with those of a modified commercial boiler. It was a floor standing boiler with a cast iron combustion chamber, designed for a nominal thermal input of 8.8 kW. Water was produced with a temperature of 70°C. This boiler had partially premixed bar burners with atmospheric injection and free entrainment of secondary air, thus creating 3-dimensional flames. This contrasts with the idealized boiler where the primary premixing is controllable and the burner slots give 2-dimensional flames. The primary aeration ratio was varied between 1.12 and 1.45, giving a total aeration ratio between 1.45 and 1.54. The combustion performance of the boiler were investigated in terms of flue gas temperature, total air factor and NO_x, and CO emissions.

Measurement Techniques

Direct visualization of the total UV/visible emission and OH, CH and C_2 emissions was achieved using an ICCD camera (Princeton Instruments) with a spatial resolution of 0.2 mm per pixel, and a camera lens (UV-Nikkor, 105 mm, f 4.5). Interference filters were used in order to select the emission wavelength from different radicals. The camera was connected to a controller (ST138, Princeton Instruments) for image acquisition and a pulse generator (DG535, Stanford Research) to synchronize the shutter and the exposure time. The camera was placed along the Z direction (see Figure 1). The exposure time varied for each flame condition and for each radical investigated. The digitized images were stored on a PC for image processing and analysis.

Fast Fourier Transform Infrared spectroscopy (FTIR) measurements of CO_2, H_2O, CO and NO and Laser Induced Fluorescence (LIF) spectroscopy measurements of OH, CH, and CN were performed in the idealized boiler for the five selected test cases. Due to space limitations, the results of these measurements will not be presented in this paper but will be discussed during the poster session of the present symposium.

Mean species (i.e., CO, CO_2, O_2, CH_4, NO and NO_x) concentrations were also measured in the combustion chamber of the idealized boiler using Sonic Nozzle Probe Sampling (SNPS). The SNPS (Pyro-Controle Chauvin Arnoux, licensed by Gaz de France) uses a suction probe with an outer diameter of 4 mm. A water cooled sonic nozzle is located at the probe tip. This nozzle is designed to quench chemical reactions in the sampled gases by fast reduction of temperature (down to about 60°C) and pressure (down to about 100 mbar of absolute pressure). The sampled gases are channeled through a heated tube maintained at 60°C, to a permeation membrane for water removal. These gases are then sent to a series of analyzers. The volumetric concentrations of CO_2 and CO are measured by infrared spectroscopy Ultramat 22P, (Siemens), CH_4 by infrared spectroscopy (Uras 4, Hartmann & Braun), O_2 by paramagnetism (Oxymat 5E, Siemens), and NO and NO_2 by

chemiluminescence (Caldos 5G, Hartmann & Braun). Prior to the measurements the analyzers were calibrated with certified standard mixtures of gases of known composition. Caution should be taken when analyzing the NO_2 measurements obtained with the probe sampling technique used here. These measurements are subject to non-trivial measurement errors particularly in flame regions of high temperature.

Temperatures were measured inside the combustion chamber by Fine Wire Compensated Thermocouples (FWCT) and Coherent Anti-Stokes Raman Spectroscopy (CARS). FWCT measurements (8) were made using two types of thermocouples (Pyro-Controle Chauvin Arnoux, licensed by Gaz de France): above Y = 20 mm, Pt-6%Rh/Pt-30%Rh thermocouples (B-type) which have a fine wire diameter of 50 µm were used, and below Y = 20 mm, Ir/Ir-40%Rh thermocouples (referred to as Ir type) which have a fine wire diameter of 80 µm were used. Ir type thermocouples can be used up to 2300 K, whereas B- type thermocouples are limited below 2000 K. The thermocouples were introduced inside the combustion chamber through a slot machined into the glass windows. The slot allows one to measure temperature along the X or Y direction, at Z = 0 mm. The thermocouples were introduced on the negative side of the X axis. The thermocouples signal was amplified (x100 to x500) with a low noise preamplifier (Stanford Research, SR-560) and digitized by a 16 bit resolution ADC board (National Instruments, AT-MIO-16-X). The temperature given by the thermocouple was numerically compensated for radiation losses (8). The thermocouples were coated with a glassy film of an inert ceramic oxide to eliminate catalytic reactions on the fine wire surface (9,10). The CARS system used an Nd:YAG laser (Continuum Powerlite 8000) which is injection seeded with a linewidth of 0.05 cm^{-1} at 532 nm and a maximum output pulse energy of 350 mJ. The modeless dye laser (ModeX) was operated with a four-pass oscillator configuration and a single amplifier. This resulted in approximately 140 mJ in the two 532 nm probe beams and 60 mJ in the dye beam. The beams were focused using a 400 mm focal length lens. This generates a control volume of approximately 200 µm in diameter and 800 µm long. The signal beam from the CARS control volume was optically filtered, collected by a 60 mm focal length lens and focused into an optical fiber. The output from the fiber was focused directly onto the input slit of the spectrometer (1.5 m SPEX, 2400 gr/mm grating). The spectrometer detector (1750x552 CCD device, Princeton Instruments) provided a resolution of 0.003 nm per pixel. At each measurement location 500 CARS spectra were recorded over a period of approximately 90 seconds.

The axial and radial velocity profiles were measured for the five selected test cases by Particle Imaging Velocimetry (PIV) and Laser Doppler Velocimetry (LDV). These measurements which, to our knowledge, have never been done in a real size household-like boiler will be presented during the poster session of the conference. The space limitations of the current paper does not allow a complete discussion on these measurements.

RESULTS AND DISCUSSION

Overall Measurements

Overall measurements were performed in the flue gases of the idealized boiler as a function of primary and secondary aeration ratio, and power input. The objective of these measurements was to determine the performances of the idealized boiler in terms of NO_x and CO emissions and to compare its behavior with that of commercially available boilers.

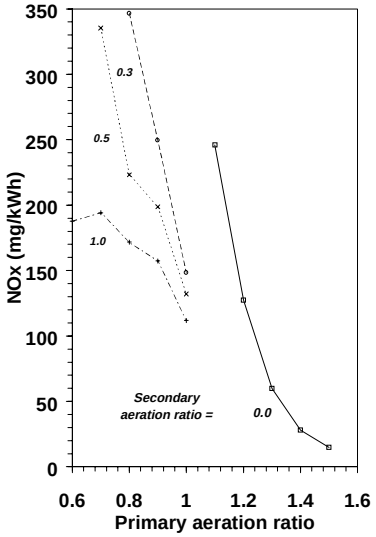

Figure 3. NOx concentration measured in the idealized boiler.

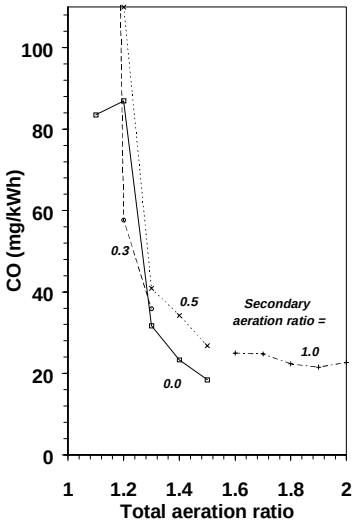

Figure 2. CO concentration measured in the idealized boiler.

Figure 2 shows the NO_x concentration measured by probe sampling in the flue gases of the idealized boiler as a function of primary aeration ratio for different secondary aeration ratios. The concentrations were obtained when the burner was operated at 10 kW. As one can see, the NO_x concentration decreases sharply when the primary aeration ratio increases. This decrease is somewhat less sharp as the secondary aeration ratio decreases. Note that very low NO_x emissions, below 50 mg/kWh) are observed with no secondary aeration, i.e., for fully premixed flames. Lean premixed flames are known to favor NO_x reduction. In these flames, the concentration of C_2, CH and CH_2 radicals are reduced, hence the attack of N_2 molecules by these radicals in the oxidation zones which is the first step for prompt NO formation (Fenimore pathway) is limited. In addition, lean premixed flames have lower temperatures, also resulting in smaller NO formation through the thermal channel (Zeldovich pathway). Figure 3 shows CO concentrations measured in the idealized boiler as a function of total aeration ratio for different secondary aeration ratios. Total aeration was selected as the X axis in this case, to stress the weak effect of secondary aeration. As one can see in Figure 3, CO emissions decrease with total aeration ratio. This decrease is almost independent of secondary aeration ratio. This shows that in the combustion chamber with enough residence time for burnout between the burner and the heat exchanger, the oxidation of CO is governed by the total availability of molecular oxygen, irrespective of whether it is provided in the primary or secondary air.

Measurements of NO_x and CO as a function of primary aeration at constant power was also obtained using a commercially available floor standing boiler. These measurements are reported in Figure 4. The strong decrease in NO_x emission with increasing primary aeration ratio as observed in the idealized boiler is evident. However, in contrast with the idealized boiler, the CO emission in the practical boiler increases sharply with primary aeration. This difference in behavior is traceable to the fact that whereas the flame in the idealized boiler blows off suddenly at a given primary aeration ratio, practical burners begin to lift long before finally blowing off. These lifted flames leak a fuel-air mixture at the edges of the burner, that is then converted to CO en route to the heat exchanger (5). These effects of primary aeration are responsible for the existence of only a narrow window in terms of operating parameters for acceptable NO_x and CO emissions.

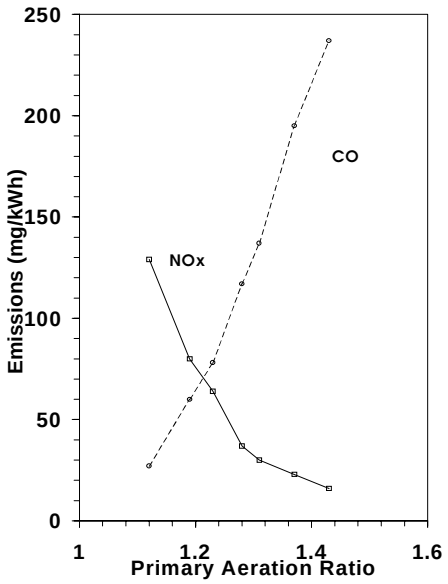

Figure 4. NO_x and CO emissions vs. primary aeration in a commercial boiler.

Emission Spectroscopy Measurements

Qualitative emission spectroscopy measurements were performed for the 5 cases selected to characterize the structure of the 5 flames. Figure 5 shows the global, OH, CH, and C_2 spontaneous emission obtained by UV/visible emission spectroscopy for Cases 1 through 5. The global emission can be considered as the sum of OH and C_2 emission since the emission of CH is weak compared to that of the others. The flame structure in Case 1 and 2 is characterized by an inner cone and two « wings ». The inner cone corresponds to the primary fuel rich flame (primary aeration ratio is 0.8), whereas the wings correspond to the secondary diffusion flame. In both cases the flame is attached to the edges of the burner slots. At this location (i.e., Y = 0 mm), the spontaneous emission is essentially due to OH and CH radicals, since the formation of C_2 is initiated only above Y = 0.8 mm. The maximum of the C_2 emission is observed at the top of the premixed reaction zone. Furthermore, C_2 is present only in the premixed reaction zone whereas OH and CH are detected also in the diffusion flame zone.

For Case 3, the emission profiles are different. The total emission profile only shows an inner fuel lean flame since no secondary air is introduced in this case. The flame appears lifted from the burner edges since the total, OH, and CH emissions only start above Y = 1.4 mm. The C_2 emission is delayed even further up and starts above Y = 2.4 mm. The OH and CH emissions are maximum at the top of the premixed flame. Case 4 and 5 which have the same primary and secondary aeration ratios present very different flame structures. The flame structure in Case 4 is very close to that of Case 3, i.e., a single premixed reaction zone is observed and no secondary diffusion flame is detected. However, in contrast with Case 3, the flame appears to be stabilized at the burner edges since both total and OH emissions start at Y = 0 mm. The flame structure in Case 5 is very different from the previous cases. As a reminder, in Case 5 an insert is placed inside the burner blades to create a V-shaped structure. The emission profiles are nearly the same for the three radicals investigated (OH, CH, C_2). They all have a V-shaped structure. The emission intensities are higher than in Case 4 and the flame surface appears larger, although the flame height is nearly the same.

Temperature Measurements

The temperatures were measured in the combustion chamber by FWCT and by CARS. Figure 6 compares the temperature profiles measured by both techniques along the centerline of the central burner slot for Case 3. As one can see, the two profiles are in good agreement. The agreement is also good for Case 4 and 5, but only fair for Case 1 and 2. Since space limitations preclude a full comparison of the results obtained with both techniques, the following discussion will focus on FWCT measurements.

The temperature maps measured by FWCT are shown below Y = 40 mm in Figure 7 for the five cases investigated. As a reminder, the FWCT measurements were obtained by introducing a thermocouple on the negative side of the X axis through a slot machined in the glass windows. Since this slot caused some flow disturbances up to about X = 0 mm, the measurements shown were performed above the slot located at X = +16 mm.

The temperature maps for Case 1 and 2 are similar and match the observations made by emission spectroscopy. The two cases only differ by the type of fuel used (synthesized natural gas like mixture vs. pure methane) and therefore have the same flame structure. If one places the flame at the location where the temperature gradient is maximum, two different flame regions are observed: above the primary channel an inner fuel rich premixed flame (primary aeration ratio = 0.6) is observed, and on both sides of the secondary air channel an outer diffusion flame develops. The maximum temperature (2290 K) is measured on both sides of the inner cone, in the region located between the premixed and diffusion flame. This corresponds to the stoichiometric reaction zone. An off-centered temperature peak is consistent with other investigations of partially premixed fuel rich flames (1). This temperature peak (i.e., 2290 K) is higher than that predicted by adiabatic equilibrium calculation (i.e., 2228 K) with an initial reactant temperature of 293 K. This superadiabatic temperature is assigned to preheating of the premixture inside of the burner slots and in the inner flame cone (1). For example, temperatures as high as 600 K were measured by thermocouples inside of the burner slots.

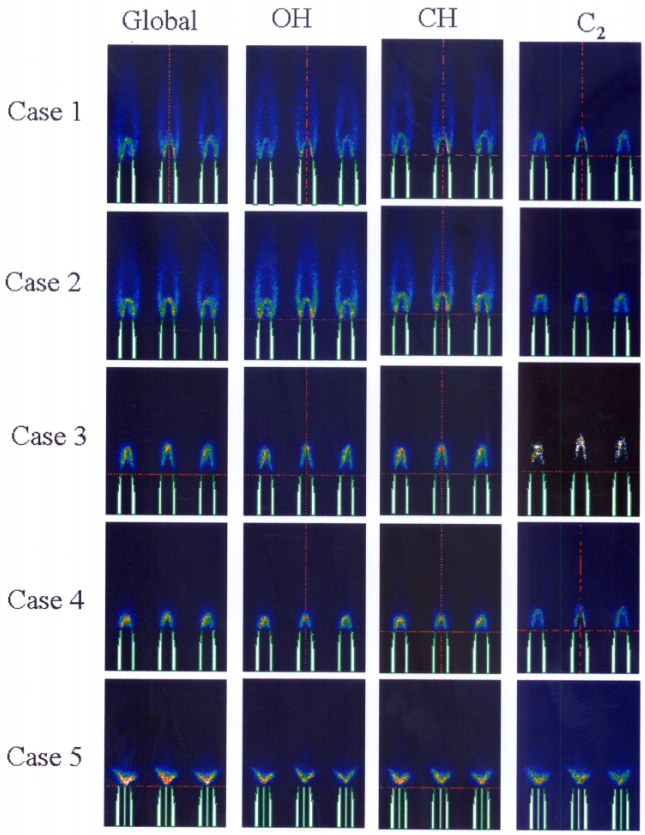

Figure 5. Total, OH, CH, C_2 spontaneous emission by UV/visible spectroscopy (arbitrary gray scale).

In Case 3 no secondary air is used, hence a fuel lean flame forms above the primary burner slot characterized by a sharp temperature gradient. As one can see in Figure 7, the temperature map is more uniform in the combustion chamber than in Case 1 and 2. The maximum temperature (i.e., 2050 K) is also higher than the adiabatic equilibrium temperature (i.e., 1857 K) for a total aeration ratio of 1.4. This is also assigned to preheating. Note that the inner flame in Case 3 is the highest of the flames investigated, thus the premixture has more time for preheating. Case 4 shows an intermediate temperature profile between Cases 1-2 and Case 3. An inner fuel lean flame (primary aeration = 1.2) forms at the burner slot. The maximum temperature (i.e., 2262 K) is measured on both sides of this inner flame. Finally in Case 5, the temperature field is as expected different from the previous cases. Sharp temperature

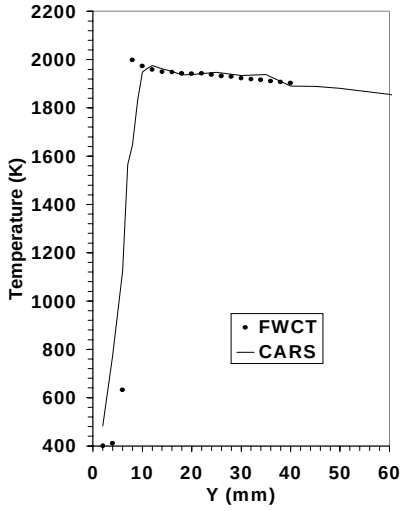

Figure 6. Centerline measurements of temperature by FWCT and CARS in Case 3.

gradients are measured on both sides of the metal insert. They corresponds to the « wings » of the V-shaped flame. The maximum temperature reached (i.e., 2295 K) is higher than in Case 4. This maximum temperature is measured above the insert.

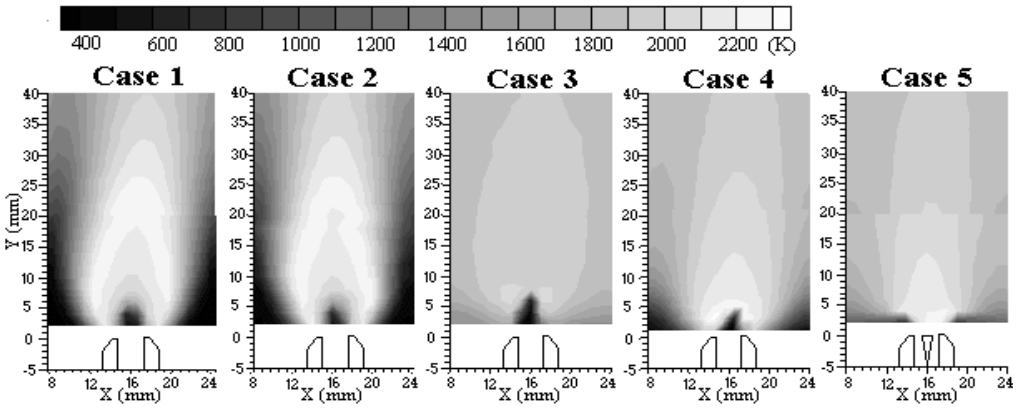

Figure 7. Temperature map measured by FWCT for Case 1 through 5.

Species Concentration Measurements

Figure 8 through 12 give the mean species concentration profiles (O_2, CO_2, CO, CH_4, NO, NO_2) measured using SNPS for Cases 1 through 5, respectively. These measurements were obtained along the centerline of the burner slot located at X = +16 mm. They are given in mole fraction (%). Note that the NO/NO_2 concentrations are magnified by 1000 for all cases except for Case 3 where they are magnified by 10000 (for reference, a mole fraction of 12.0 % on the left axis corresponds to a NO concentration of 12 ppm in case 3, and 120 ppm in all other cases). The mean species mole fractions are shown up to Y = +60 mm since they do not evolve significantly further up. The corresponding temperature profiles measured using FWCT along the same centerline are shown also for each flame case (the temperature axis is given on the secondary Y axis).

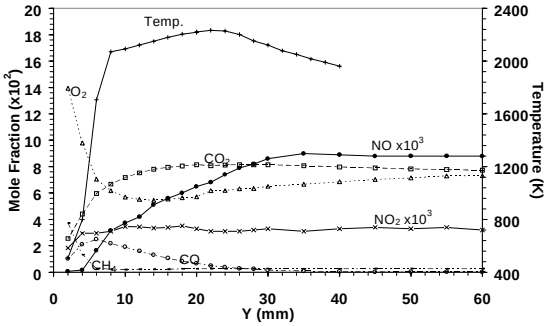

Figure 8. Axial profiles for flame case 1.

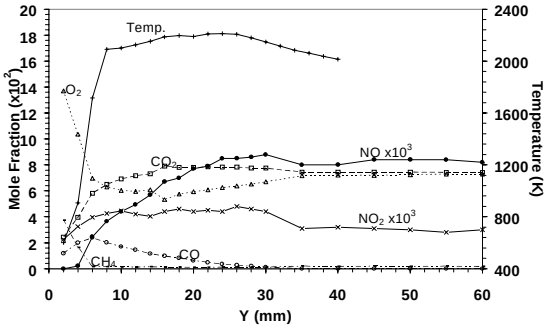

Figure 9. Axial profiles for flame case 2.

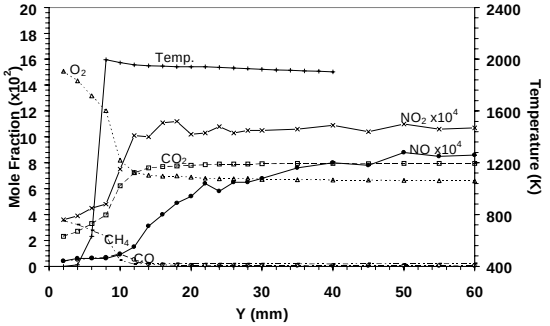

Figure 10. Axial profiles for flame case 3.

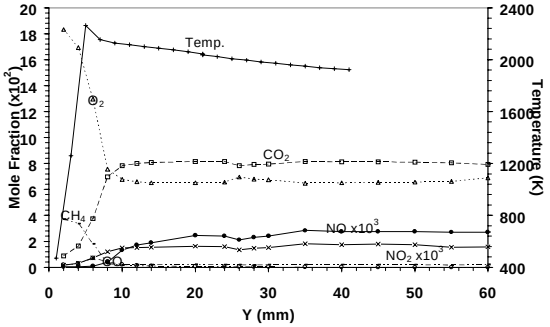

Figure 11. Axial profiles for flame case 4.

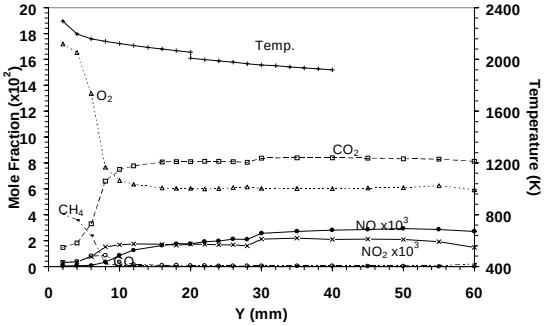

Figure 12. Axial profiles for flame case 5.

The mean species concentration profiles are similar for Case 1 and 2 as expected from temperature and emission spectroscopy measurements. In both cases, the maximum CO concentration measured corresponds to the location where the temperature gradient is maximum, which is assigned to the location of the inner premixed flame. The NO concentration profiles follow the same trend and can be divided in three stages: a stage of sharp concentration increase is observed from the burner mouth up to the location of the CO concentration peak (i.e., the location of the inner flame); a stage of gradual concentration increase follows, up to the location where the temperature is maximum (i.e., Y = 24 mm); finally above this location, the NO concentration remains almost constant up to Y = +60 mm. At Y = +60 mm, the NO and NO_2 concentrations are 90 and 30 ppm, respectively, which corresponds to their respective concentrations in the flue gases. The stage of sharp concentration increase can be assigned to NO formed through the prompt (Fenimore) pathway. At the end of this stage, the NO_x concentration (taken as [NO]+[NO_2]) represents half of the total NO_x produced (i.e., the NO_x concentration is 60 ppm at Y = 8 mm). This, however, does not take into account the dilution with secondary air. The stage of gradual increase, which starts around

Y = 8 mm at a location where the temperature is above 2000 K, is likely to be due to the formation of thermal NO (Zeldovich pathway). At this temperature level, the Zeldovich pathway is known to have an important contribution (11). The NO_2 concentration remains constant throughout the combustion chamber although a slight increase is noticeable at the early the stage of the gradual increase. At Y = 60 mm, NO_2 represents only about 25% of the total amount of NO_x produced.

The mean species concentration profile for flame Case 3 is shown in Figure 10. In this case, the flame is a Bunsen like fuel lean fully premixed flame since no secondary air is used. The NO concentration slowly rises from the burner surface to about Y = 8 mm. This slow rise which is assigned to NO produced through the Fenimore pathway is in striking contrast with the corresponding sharp increase observed in Case 1 and 2. At the end of this rise, i.e., Y = 8 mm, the NO concentration represents only 25% of the total amount of NO produced. As discussed previously in the overall measurements, fuel lean flames show lower concentrations of CH radicals than their fuel rich counterparts. Hence, the concentration of NO produced which is sensitive to the CH-HCN reaction pathway in the Fenimore mechanism (11), remains low. From Y = 8 mm to Y = 20 mm, the NO concentration increases sharply. This is most likely due to the Zeldovich mechanism with contribution from superequilibrium O atoms. At these locations, the maximum temperature is 1997 K. Therefore, the total NO_x concentration increases up to 20 ppm. The NO_2 concentration is almost constant up to Y = 8 mm. However, it increases significantly between Y = 8 mm and Y = 20 mm. At Y = 60 mm, NO_2 represents about 50% of the total NO_x produced. Note that this high concentration could be due to an artefact of the measurement technique. In both Case 4 and 5, the concentration profiles are similar to those observed in Case 3 in terms of NO and NO_2. However, since both flames are shorter than in Case 3, the slow rise assigned to the formation of NO through the Fenimore mechanism ends lower in the combustion chamber (i.e., Y = 6 mm). The maximum flame temperature in Case 4 and 5 (i.e., 2262 K and 2295 K, respectively) is higher than in Case 3, therefore the total NO_x measured at Y = 60 mm is higher (about 50 ppm in both cases). The NO_2 concentration represents about 40% of the total amount of NO_x produced, which leads to the conclusion that the relative amount of NO_2 produced increases with increasing primary aeration ratio.

CONCLUSIONS

Preliminary results of the experimental investigation of an idealized boiler were presented. They represent one of the most complete set of experiments aimed at understanding the combustion processes in a real size household boiler. They show how one can use advanced measurement techniques in a real practical appliance, to study pollutant formation mechanisms. These results are very valuable in providing insights into how burner operation affects emission performances. They will therefore represent the basis for the boiler Design Guidelines that will be delivered as part of the TOPDEC project. Finally, they represent a complete database for the validation of numerical predictions.

ACKNOWLEDGMENTS

The results of this project are published by kind permission of Companies, Universities and Organizations which are involved in TOPDEC, and of the European Commission which financial contribution to this project is gratefully acknowledge.

REFERENCES

1. Nguyen, Q.V., Dibble, R., Carter, C.D., Fiechtner, G.J. and Barlow R.S. (1996). Raman-LIF Measurements of Temperature, Major Species, OH, and NO in a Methane-Air Bunsen Flame. *Combustion and Flame*, 105:499-510.
2. Van Oostendorp, D.L., Borghols, W. T. A., and Levinsky, H. B. (1991). The influence of Ambient Air Entrainment on Partially Premixed Burner Flames: LIF Imaging of CO and OH. *Combustion and Flame*, 79:195-206.
3. Arrigotti, S., Bernstein, S., Levinsky, H.B., Van Oostendorp, D.L., and van der Meij, C.E. (1992). Numerical and Experimental Investigation of a Laminar Bunsen Flame. *Proceedings 1992 International Gas Research Conference*, Orlando, FL, 1753-1762.
4. Hasko, S.M., Fairweather, M., Bachman, J.S., Imbach, J., van der Meij, C.E., Mokhov, A.V., Jacobs, R.A.A.M. and Levinsky, H.B. (1995). Optical-Diagnostic and Numerical Study of an Experimental Slot Burner. *Proceedings 1995 International Gas Research Conference*, Orlando, FL, 33-42.
5. Van der Meij, C.E., Mokhov, A.V., Jacobs, R.A.A.M. and Levinsky, H.B. (1994). On the Effect of Fuel Leakage on CO Production from Household Burners as Revealed by LIF and CARS. *Twenty-Fifth Symposium (International) on Combustion*, The Combustion Institute 243-250.
6. Levinsky, H.B., van Oostendorp, D.L., van der Meij, C.E., Jacobs, R.A.A.M. and Mokhov, A.V. (1992). Pollutant Formation in Household Burners: LIF Imaging of NO. *Proceedings 1992 International Gas Research Conference*, Orlando, FL, 1578-1586.
7. Joos, L. (1995). State of the Art in Pollution Control for Gas Appliances. Proceedings *6th International Gas Congress (IRGUC)*, Prague, Czech Republic.
8. Neveu, F., Corbin, F., Perrin, M. and Trinité, M. (1995). Characterization of the couplings of aerodynamics and combustion in a nonpremixed turbulent flame. *Rev. Gén. Therm.*, 34:305-314.
9. Shandross, R.A., Longwell, J.P. and Howard, J.B. (1991). Noncatalytic Thermocouple Coating for Low-Pressure Flames. *Combustion and Flame*, 85:282-284.
10. Kent, J.H. (1970). A Noncatalytic Coating for Platinum-Rhodium Thermocouples. *Combustion and Flame*, 14: 279-282.
11. Muzio, L.J. and Quartucy, G.C. (1997). Implementing NOx Control: Research to Application. *Prog. Energy Combust. Sci.*, 23:233-266.